

Non-Newtonian Blood Flow in Left Coronary Arteries with Varying Stenosis: A Comparative Study

PoojaJhunjunwala¹, P.M. Padole²and S.B. Thombre³

Abstract: This paper presents Computational fluid dynamic (CFD) analysis of blood flow in three different 3-D models of left coronary artery (LCA). A comparative study of flow parameters (pressure distribution, velocity distribution and wall shear stress) in each of the models is done for a non-Newtonian (Carreau) as well as the Newtonian nature of blood viscosity over a complete cardiac cycle. The difference between these two types of behavior of blood is studied for both transient and steady states of flow. Additionally, flow parameters are compared for steady and transient boundary conditions considering blood as non-Newtonian fluid.

The study shows that the highest wall shear stress (WSS), velocity and pressure are found in artery having stenosis in all the three branches of LCA. The use of Newtonian blood model is a good approximation for steady as well as transient blood flow boundary conditions if shear rate is above 100 s^{-1} . However, the assumption of steady blood flow results in underestimating the values of flow parameters such as wall shear stress, pressure and velocity.

Keywords: Left coronary artery, computational fluid dynamics, non-newtonian, plaque, transient.

1 Introduction

Computational Fluid Dynamics (CFD) is a branch of Fluid Mechanics which helps in predicting fluid flow, mass transfer, heat transfer etc. related phenomena of complex bodies by solving governing non-linear mathematical equations using a numerical process. Recently, CFD has gained popularity in biomedical research of cardiovascular related problems. Since, in-vivo measurements for quantification of the hemodynamic of healthy and stenosed arteries are complicated and expensive, CFD is a very useful tool for studying such type of artery flows [Govindaraju, Badruddin, Viswanathan, et al.,

¹ Department of Mechanical Engineering, VNIT, Nagpur, India

Pooja Jhunjunwala- +91-8149884920; pooja.jjw@students.vnit.ac.in

² Department of Mechanical Engineering, VNIT, Nagpur, India

P. M. Padole- +91-9822220713; pmpadole@mec.vnit.ac.in

³ Department of Mechanical Engineering, VNIT, Nagpur, India

S.B. Thombre- +91- 9422803441; sbthombre@mec.vnit.ac.in

(2013)]. The flow parameters like wall shear stress (WSS), velocity and pressure distributions can be obtained through CFD simulations for both steady and transient states [Johnston, Johnston, Corney, et al., (2006), Perktold, Hofer, Rappitsch, et al., (1997)]. These results can help doctors to improve clinical decisions.

In the present world, Coronary artery disease (CAD) is major cause of death and morbidity [Sun and Xu(2014)]. This is an inflammatory disease with plaque deposition in the wall of arteries [Hansson (2005)]. It is known from clinical practice that specific locations in coronary arteries are prone to the development of stenosis (plaque deposition). Left coronary bifurcation is the most common site for plaque origination [Chaichana, Sun and Jewkes (2011)]. Local haemodynamics plays an important role in the origination and development of these plaques at left coronary bifurcation [Gijssen, van de Vosse and Janssen (1999)]. Wall shear stress, pressure distribution, velocity distribution, secondary flow and flow separation have crucial role in growth and origination of stenosis [Govindaraju, Badruddin, Viswanathan, et al., (2013)]. The stenosis is predominant at bends and bifurcation as it results into disturbance in bloodflow, creation of secondary flow and flow separation [Wellnhofer, Osman, Kertzscher, et al., (2010)]. Hence, in the present work, the effects of different types of stenosis in a left coronary artery (LCA) on flow parameters such as WSS, velocity and pressure distribution have been analysed under different boundary conditions. Chaichana, Sun and Jewkes [Chaichana, Sun and Jewkes (2013)] have made haemodynamic analysis of the effects of different types of plaques in LCA assuming blood as a Newtonian fluid. However, it is known that blood is a shear thinning fluid and hence it needs to be considered as a non-Newtonian fluid.

Many previous works have been done assuming blood as a Newtonian fluid, giving argument that in large arteries, shear rates are high and blood behaves as a Newtonian fluid if shear rate is greater than 100 s^{-1} [Gijssen, van de Vosse and Janssen (1999)]. Johnston, Corney and Kilpatrick [Johnston, Johnston, Corney, et al., (2004)] have suggested that for flow velocities in steady state simulations, non-Newtonian effects are important. However, for unsteady flow in coronary arteries, there is no consensus in the literatures on importance of effects of non-Newtonian model of blood. On one hand some studies [Gijssen, Vosse and Janssen (1999), Deville(1996)] claim non-Newtonian rheology to be important, on the other hand some studies [Ballyk, Steinman and Ethier (1994), Johnston, Johnston, Corney, et al., (2006)] found it relatively unimportant. The present study, therefore, has been made for both models (Newtonian and non-Newtonian) of blood under steady as well as transient state of flow.

The aims of this research work are:

- To study the results of flow parameters in a complete cardiac cycle for three different (idealized 3-D) models of LCA.
- To compare the results derived by Newtonian and non-Newtonian (Carreau) models of blood for steady state as well as transient state separately.
- To compare the results of non-Newtonian model of blood for steady and transient state, so as to study the justification for assumption of steady state flow.

In the present study, the artery walls have been assumed to be rigid, smooth and impermeable. Although, it is known that actual artery walls are irregular and elastic in

nature because of which alteration in geometry during a cardiac cycle occurs. Also in this work, flow is simulated on a fixed mesh, but it is also known that coronary artery moves during a cardiac cycle. However, Santamarina, Weydahl, Siegel and Moore [Santamarina, Weydahl, Siegel, et al., (1998)] mentioned in their work that no significant change in velocity is observed due to movement of coronary artery if its frequency is up to 1 Hz. Hence, these assumptions can be made as it may not significantly influence the obtained results.

2 Materials and methods

2.1 Geometry modeling and mesh generation

In order to compare the effects of plaque deposition (stenosis) on the flow parameters inside the left coronary artery (LCA), three different models - healthy LCA (artery A), LCA having stenosis at single location (artery B) and LCA having multiple stenosis (artery C) are modeled as shown in Fig. 1. Many earlier research papers have stated complex flow in certain locations of arteries leads to deposition of plaque. Branching, bifurcation and curvature of arteries causes complex flow in arteries [Valencia, Solis (2006)]. Deposition of plaque in LCA is most common at location where it gets bifurcated [Sun, Cao (2011)]. It is also supported by clinical results. Therefore, plaque deposition in models B and C are made in accordance with the previous literatures and clinical practice. In some literatures [Pericevic, Lally, Toner, et al., (2009)], it is mentioned that geometry of artery can be assumed to be almost tubular and symmetrical. In the present work, 3-D models of LCA are modeled with this assumption. All three models are constructed in SolidWorks (a commercial 3D CAD software). The length and diameter of LCA before bifurcation (LMS) are considered to be 8 mm and 5 mm respectively as per the clinical values. The length of LCA after bifurcation i.e. of LAD (Left Anterior Descending) and LCx (Left Circumflex) both is 16 mm. However, diameter of LAD is 3 mm and that of LCx is 2mm. The bifurcation angle is 60°. The geometries of all three models are nearly same. The only difference between these is reduction in volume due to stenosis near point of bifurcation at single location in artery B and multiple locations in artery C. In artery B, the deposited plaque is assumed to be circular and symmetrical. However, in artery C plaque deposition at distal wall of LAD is noncircular.

The 3-D CAD models are imported into pre-processing program for mesh generation (ANSYS v 14.5). The models A, B and C are discretized into 141699, 146898 and 1000770 elements respectively. Meshes were further refined to perform grid independency test. The relative errors in the results were negligible. However, further refinement of mesh is neglected in order to save the computational time.

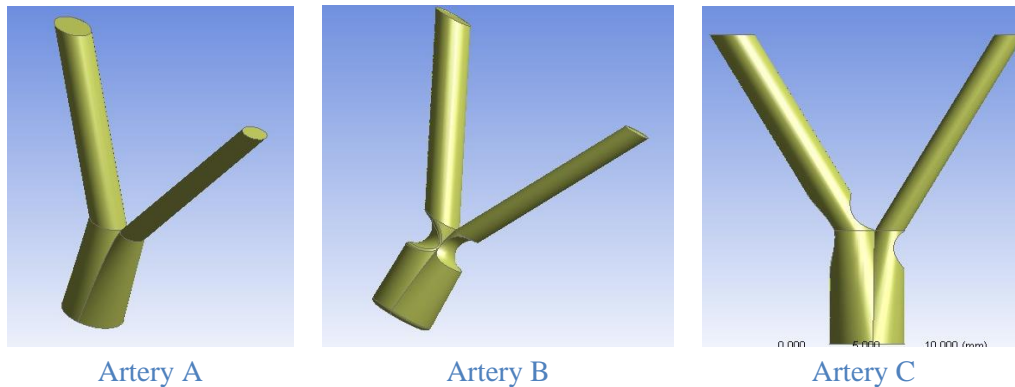


Figure 1:3-D models of left coronary artery.

2.2 Fluid properties and boundary conditions

The flow conditions in the LCA are studied assuming blood to be incompressible and homogeneous fluid with density $\rho = 1060 \text{ kg/m}^3$ [Karimi, Dabagh, Vasava, et al., (2014)]. The flow is assumed to be laminar as in [Valencia, Solis (2006), Banks, Bressloff (2007)] since, the average Reynolds number in the present work ranges from 150 to 800.

One of the objectives of the present work is to decide the velocity range for which blood can be assumed as a Newtonian fluid. In order to do so, two different simulations are made for each boundary conditions. In first simulation, blood is assumed to be a Newtonian fluid having viscosity of 0.0035 kg/ms as in [Jeong, Jaehoon (2014)].

Johnston, Johnston, Corney and Kilpatrick [Johnston, Johnston, Corney, Kilpatrick (2004)] have suggested to use Generalized Power law to incorporate non-Newtonian behavior of blood in numerical studies of artery but also stated that Carreau model can also be used with fairly good accuracy. The other authors like Kehrwald [Kehrwald (2005)] have also suggested to use Carreau model for simulation of blood flow. Hence, in second simulation, blood is considered as non-Newtonian fluid following Carreau model. As per Carreau model [Cho, Kensey (1991)]:

$$\mu - \mu_{\infty} = (\mu_0 - \mu_{\infty}) \left(1 + (\lambda \dot{\gamma})^2\right)^{\frac{n-1}{2}} \quad (1)$$

where $\lambda = 3.313 \text{ s}$, $n = 0.3568$, $\mu_0 = 0.056 \text{ kg/ms}$ & $\mu_{\infty} = 0.0035 \text{ kg/ms}$. These values are fitted from the experimental data [Cho, Kensey (1991)]. Here μ_0 & μ_{∞} are the dynamic viscosities at zero and infinite shear rate respectively. μ is the effective viscosity. $\dot{\gamma}$, λ and n are representing shear rate, characteristic viscoelastic time of the fluid and power law index respectively.

The CFD study is based on the continuity and momentum equations. It is assumed that blood flow in LCA is governed by Navier- Stokes equation:

$$\rho \left[\frac{\partial \mathbf{v}}{\partial t} + (\mathbf{v} \cdot \nabla) \mathbf{v} \right] = -\nabla \tau - \nabla p \quad (2)$$

and Continuity equation:

$$\nabla p = 0 \quad (3)$$

for incompressible fluid.

In the above equations, \mathbf{v} is 3-dimensional velocity vector, ρ is density, t is time, τ is stress tensor and p is the pressure. Writing Navier-Stokes equation in the form of stress tensor gives the flexibility to use any non-Newtonian model. These highly non-linear governing equations are solved numerically using finite volume method (FVM) as implemented in the software package ANSYS FLUENT v 14.5 for CFD related problems.

A set of boundary conditions are required for solving the governing equations. The solid walls of the LCA models are assumed to be rigid as in Johnston, Johnston, Corney and Kilpatrick [Johnston, Johnston, Corney et al., (2006)]. The no-slip condition is imposed on velocities of artery walls. At the outlets of artery, the gauge pressure is set to 100 mm Hg (mean of normal systolic and diastolic pressure). Physiologically, blood flow inside artery is pulsatile in nature. At the inlet of the artery, a uniform time-varying velocity profile [Jhunjhunwala, Padole and Thombre (2015)] as shown in Fig. 2 is imposed to include pulsatile flow in the simulation. The flow pattern of sinusoidal wave during systole [Sinnott, Clearly and Prakash (2006), He, Duraiswamy, Frank et al., (2005); Duraiswamy, Schoepfoerster and Moore (2009)] is used as an approximation to physiological pulse. Diastole phase in the assumed velocity profile represents cut-off of supply from the heart having constant velocity of 0.1 m/s. The assumed velocity wave form yields a maximum inlet velocity of 0.5 m/s with a rapid heartbeat (during exercise) of 120 per minute. The duration of a complete cycle is 0.5s. The uniform-transient velocity profile at the inlet is defined in the software by user defined function (UDF). To compare Newtonian and non-Newtonian models of blood for steady flow, a constant inlet velocity of 0.36 m/s [Owega, Klingelhofer, Sabri et al., (1998)] is assumed.

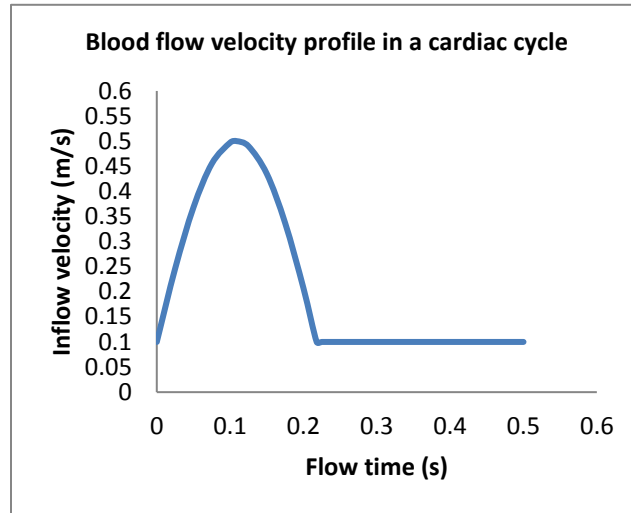


Figure 2: Blood flow velocity profile into LCA

The used CFD code utilizes a solver of implicit formulation. The 'SIMPLE' algorithm is selected for the pressure-velocity coupling. For spatial discretization of pressure, Standard technique is used. Second Order Upwind discretization method is applied for momentum equations. The transient flow analysis is conducted with time step size of 0.01 s. Two cycles (100 time steps) are required to achieve a period independent solution. Therefore, results of the second cycle are only presented in the result section. The convergence criterion (difference between two consecutive iterations) is 10^{-4} for all equations since it gives satisfactory result for each time step.

3 Results and discussion

3.1 Analysis of flow parameters in the three artery models

A set of plots of flow parameters (velocity, pressure and WSS) for each of the three LCA models were obtained for the non-Newtonian model (Carreau) of blood under transient state at various time instances. As an illustration, Figs. 3-5 contains plots of velocity, pressure and WSS respectively for the three arteries at $t = 0.55$ s. If these are studied, flow parameters can be compared in the three models.

3.1.1 Description of velocity inside the LCA

In the velocity vector plot (Fig. 3), the velocity values ranged from 0 m/s to 2.4 m/s corresponding to five contour levels, approximately 0.5 m/s at per level. Fig. 3 (b & c) shows the region of high velocities, ranging from 1.64 m/s to 2.4 m/s at the stenotic locations in the yellow and red contour levels. Artery B had the plaques located in the LMS (left main stem), so the high velocity was observed at the stenotic regions of LMS. Artery C had stenosis in the regions of LMS, LAD and LCx branches, so high velocity

was observed at the stenosed locations of these branches of LCA in the plot. However, velocity is also high downstream of stenosis which eventually gets reduced as blood flows forward in both artery B and C. It shows flow reversal occurs (due to recirculation) downstream the plaque locations in the two stenosed models (B & C) which does not occur in case of artery A (healthy artery).

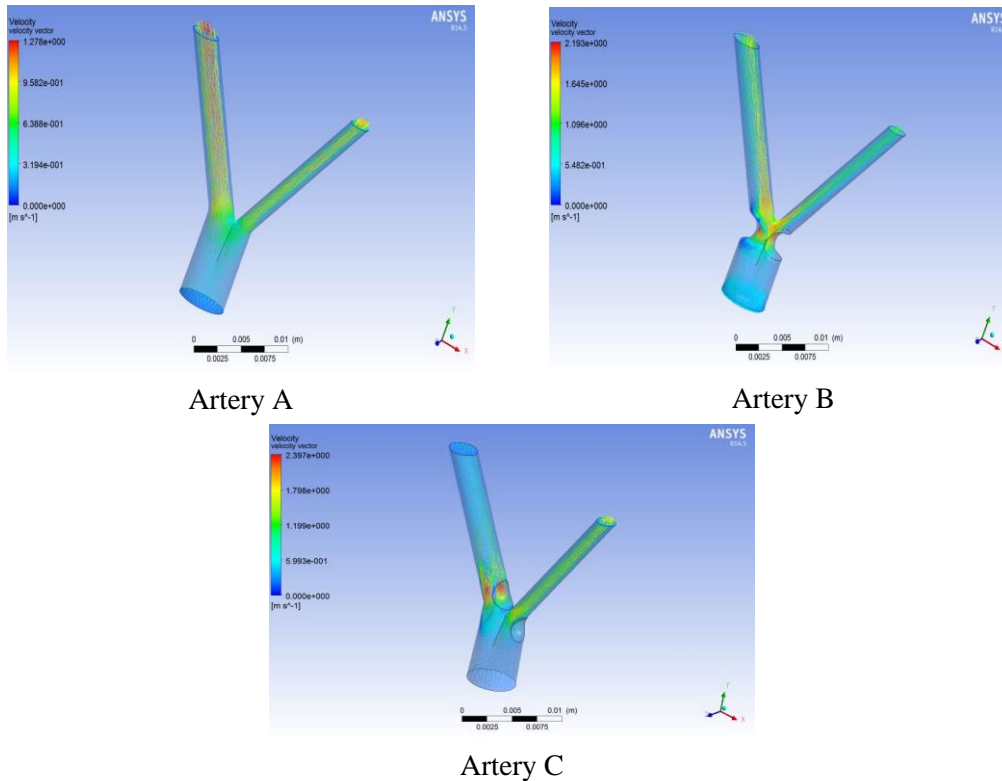
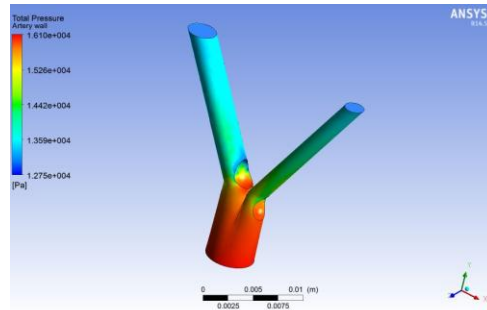


Figure 3: Velocity distribution at $t = 0.55$ s

3.1.2 Description of pressure inside the LCA

The pressure contour plot (Fig. 4) indicates the pressure ranges from 12748 Pa to 16099 Pa, corresponding to 5 contour levels. The high pressure region in all three models is at the point of bifurcation and near entrance which extends downstream with the growth of stenosis and increase in velocity within a cardiac cycle. It is due to the fact, that flow does not have stagnation point in stenosed artery [Valencia A., Solis F. (2006)]. In the post stenotic regions, pressure gets reduced.

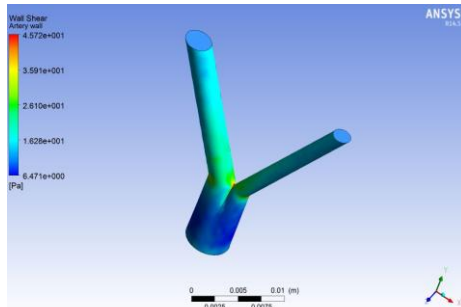


Artery C

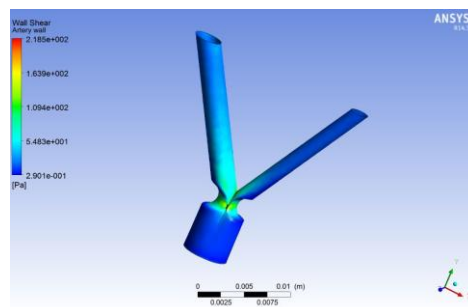
Figure 4: Pressure distribution at $t = 0.55$ s

3.1.3 Description of WSS inside the LCA

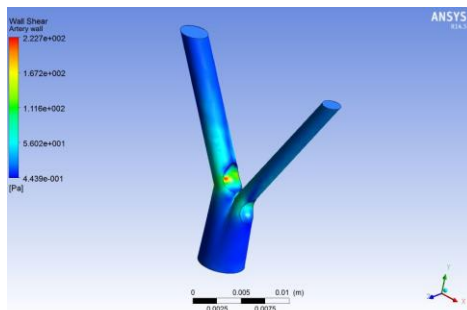
The WSS ranges from 0 Pa to 223 Pa as shown in Fig. 5. The high WSS ranging from 164 Pa to 223 Pa lies in the stenotic regions [Fig. 5 (b & c)]. WSS is minimum near the entrance which reaches its maximum at stenotic regions and gradually decreases downstream the flow. Wall shear stress is maximum at the point of bifurcation for artery A {Fig. 5 (a)}. This, in fact is responsible for the development of growth of stenosis near bifurcation region [Jhunjhunwala, Padole andThombre. (2015)].



Artery A



Artery B



Artery C

Figure 5: Wall shear stress distribution at $t = 0.55$ s

3.1.4 Variation of flow parameters for a cardiac cycle

The maximum values attained by velocity, pressure and WSS over a cardiac cycle for the three models are shown in Figs. 6-8. It is observed that, the maximum values of flow parameters increase and reaches its peak at peak value of systole while wave form is accelerating, then decreases (during decelerating phase) and becomes constant in diastole. It shows that during a cardiac cycle, there is continuous variation in hemodynamic parameters which will eventually affects the physiology of blood. A drastic increase (maximum for artery C) in values of flow parameters can also be observed from Figs. 6-8, which shows it is important to study arteries having different types of plaques with varying percentage of stenosis.

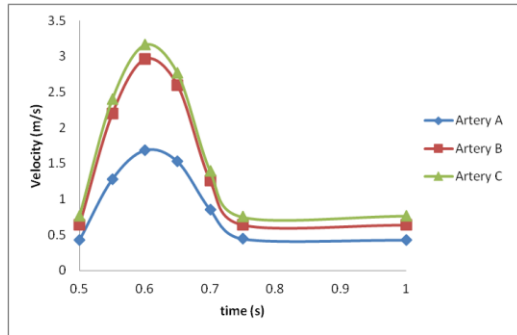


Figure 6: Variation in maximum velocity during a cardiac cycle

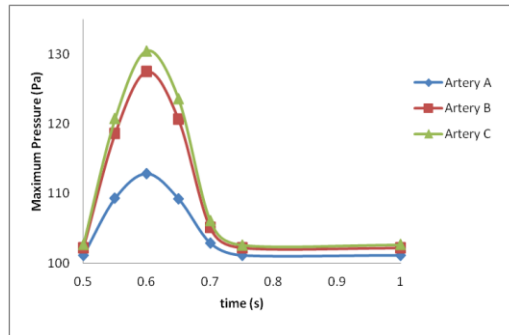


Figure 7: Variation in maximum pressure during a cardiac cycle

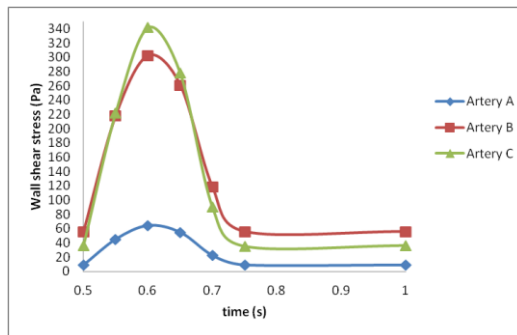


Figure 8: Variation in maximum wall shear stress during a cardiac cycle

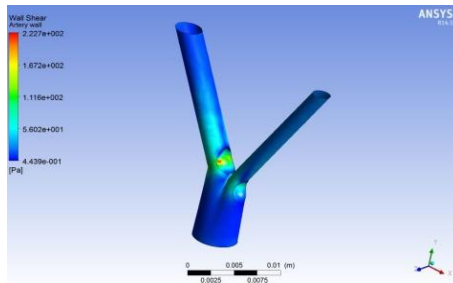
3.2 Comparison of flow parameters

For each of the three geometric models of left coronary artery and for the two blood viscosity models (described in section 2.2), series of simulations were performed separately under steady as well as transient states. However, same trend in results were observed for all the three left coronary arteries. Therefore, for comparison purpose of different models of blood and flow, results of only artery C have been illustrated in the subsequent sections. Artery C is selected because it represents the worst physiological conditions.

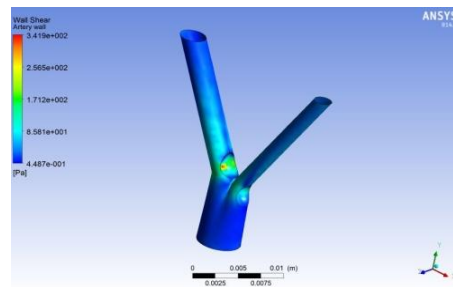
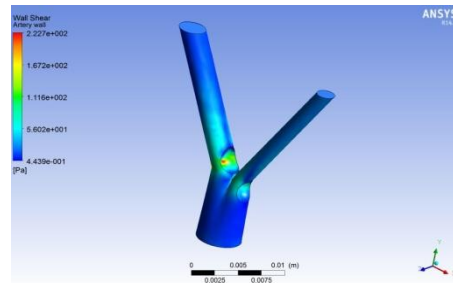
3.2.1 Newtonian vs non-Newtonian model for transient flow

The WSS, velocity and pressure distribution contour plots of artery C for Carreau blood viscosity and Newtonian models are shown in Figs. 9-11 respectively. Distributions are presented at the time instants of 0.55 s, 0.6 s, 0.65 s, 0.7 s, 0.75 s and 1 s within the cardiac cycle. Results at these time instants were chosen as they represent:

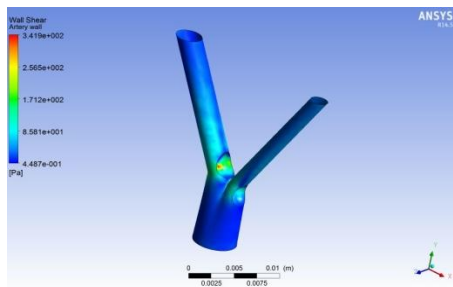
- $t_1 = 0.55$ s, middle of the accelerating phase of systole
- $t_2 = 0.6$ s, peak of systole
- $t_3 = 0.65$ s, middle of the decelerating phase of systole
- $t_4 = 0.7$ s, just before onset of diastole
- $t_5 = 0.75$ s, initial diastolic phase
- $t_6 = 1$ s, end of cardiac cycle

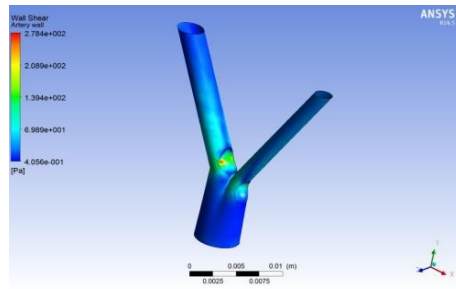


$t = 0.55$ s

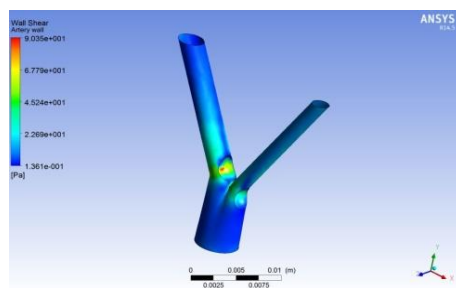
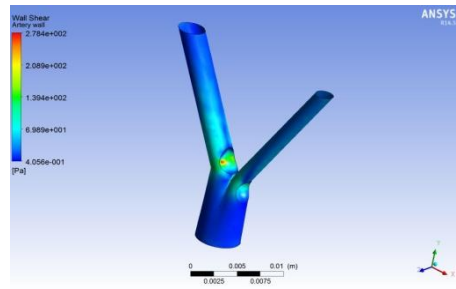


$t = 0.6$ s

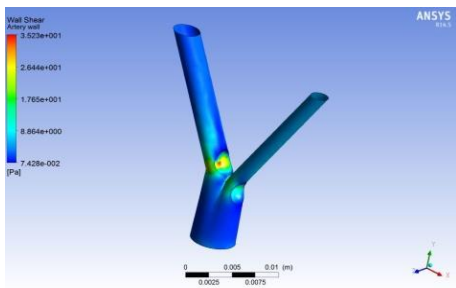
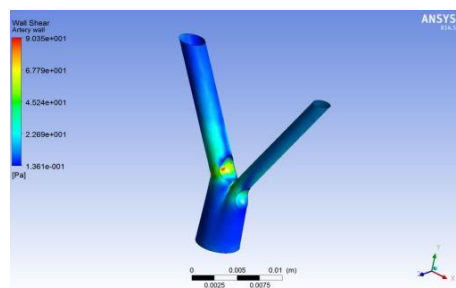




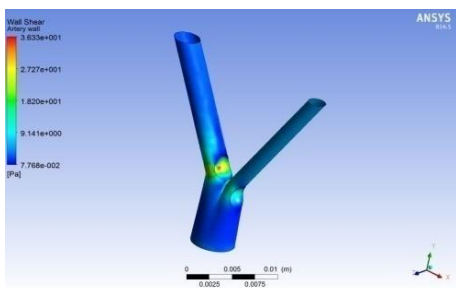
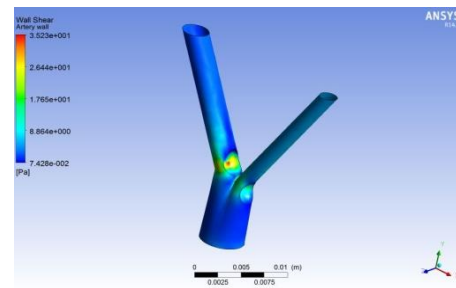
$t = 0.65 \text{ s}$



$t = 0.7 \text{ s}$

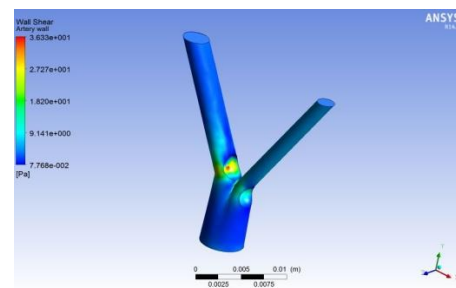


$t = 0.75 \text{ s}$



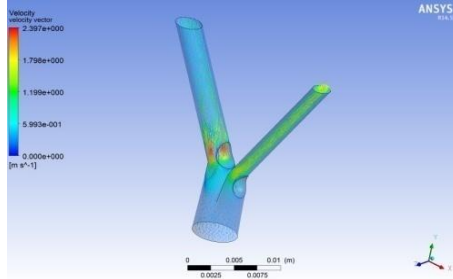
$t = 1 \text{ s}$

(a)

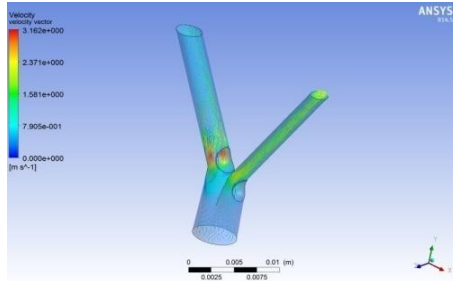
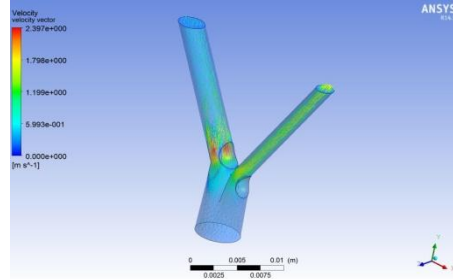


(b)

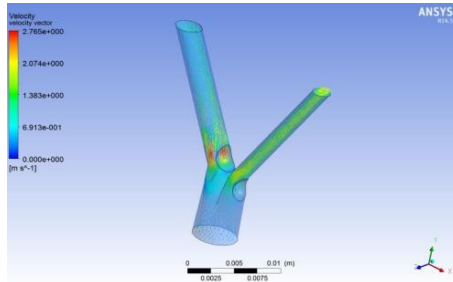
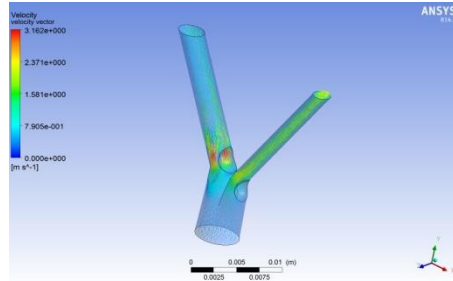
Figure 9: Distribution of wall shear stress in artery C at different time instants of transient state simulations for (a) Newtonian (b) non-Newtonian models of blood



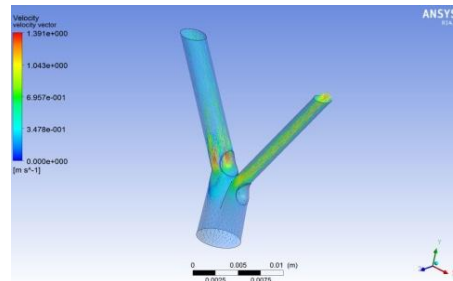
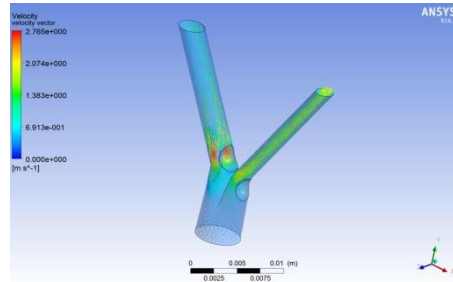
$t = 0.55 \text{ s}$



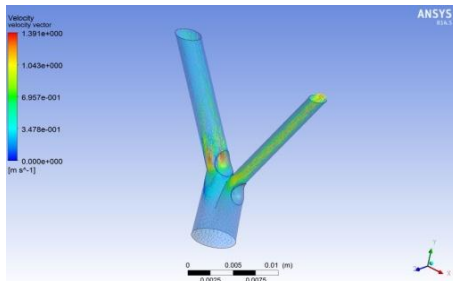
$t = 0.6 \text{ s}$



$t = 0.65 \text{ s}$



$t = 0.7 \text{ s}$



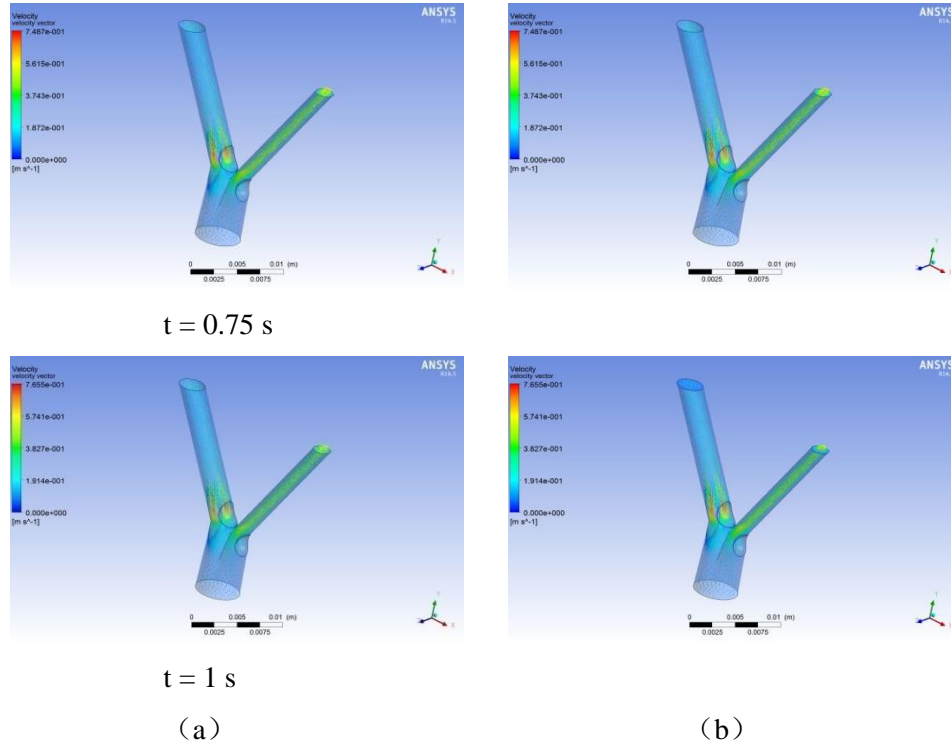
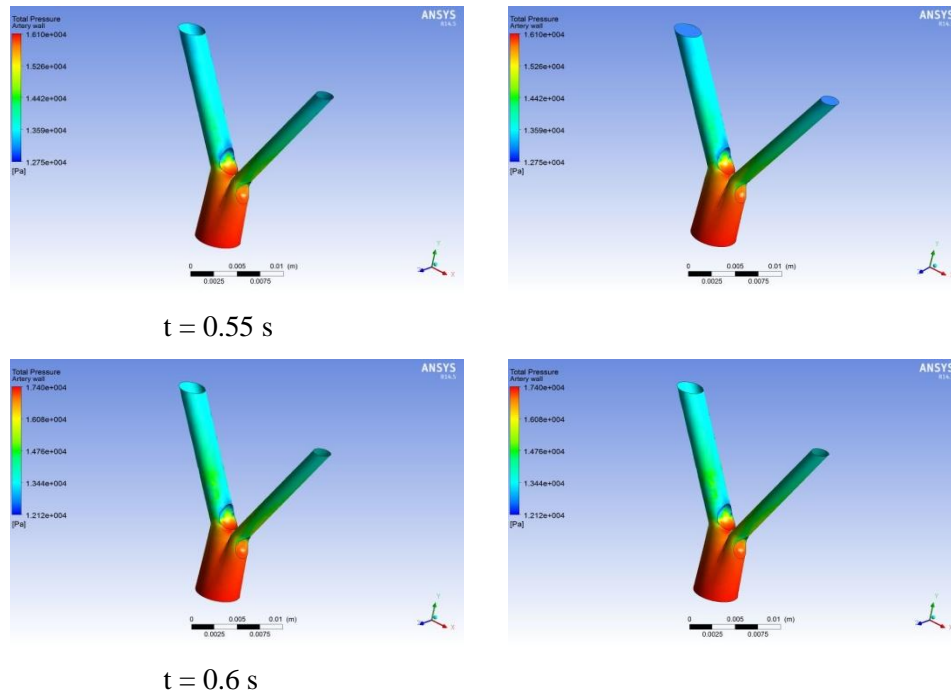


Figure 10: Distribution of velocity in artery Cat different time instants of transient state simulations for (a) Newtonian (b) non-Newtonian models of blood



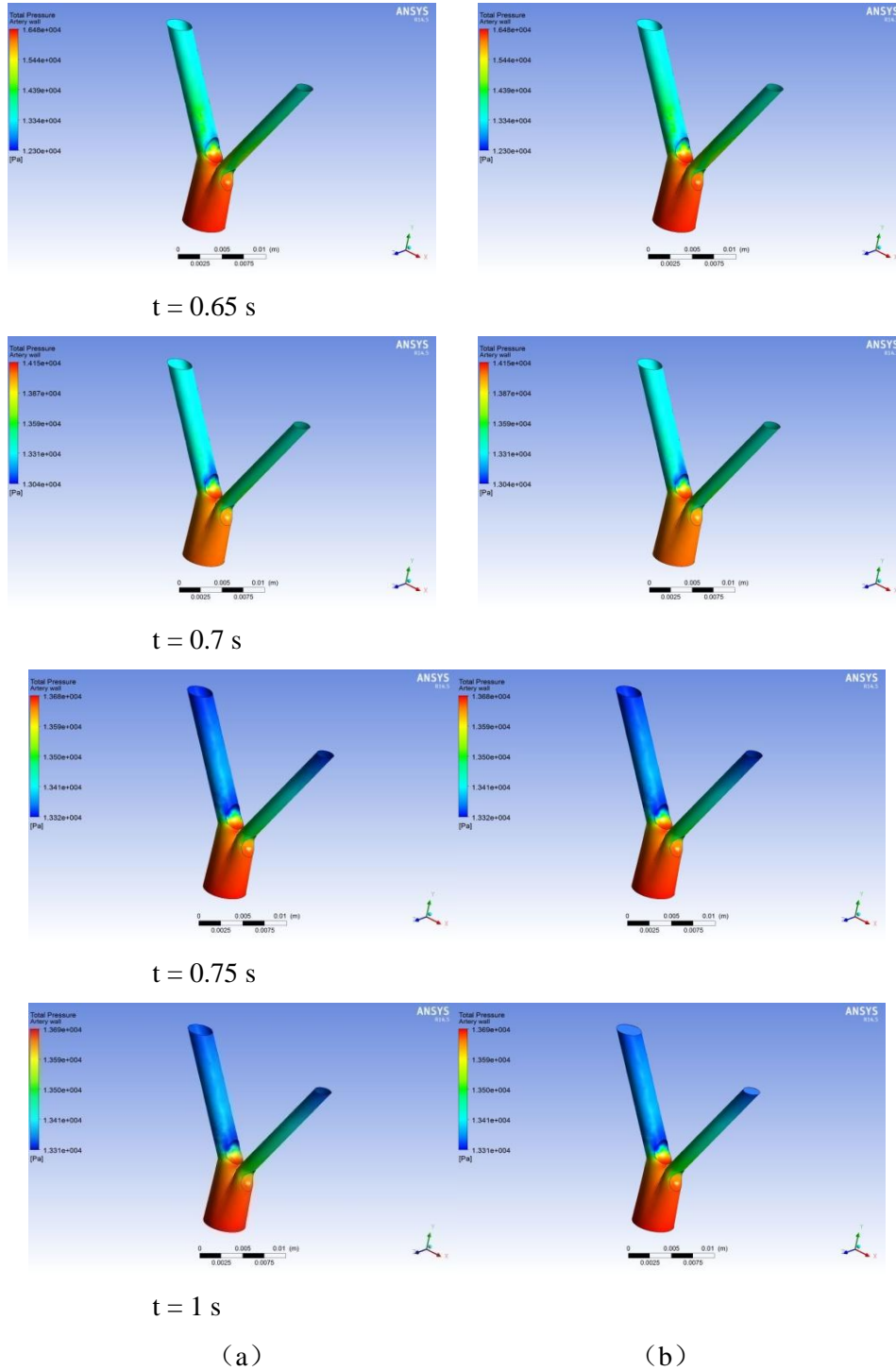


Figure 11: Distribution of pressure in artery Cat different time instants of transient state simulations for (a) Newtonian (b) non-Newtonian models of blood

It can be observed from the Figs. 9-11, that there is almost no visual difference in WSS, velocity and pressure distributions between the two blood viscosity models of LCA throughout the cardiac cycle. The inlet velocity throughout the cardiac cycle ranges between 0.1 -0.5 m/s. The maximum value reached by these flow parameters at above mentioned time instants are presented in Table 1. Evidently, quantity wise there is no difference in the two blood models under transient state which is in close agreement with the results of [Johnston, Johnston, Corney, et al., (2006)].

Table 1: Maximum values attained by flow parameters in artery C for the two blood models at different time instants of transient state simulation

Time (s)	Artery C					
	Newtonian			Non-Newtonian		
	Velocity (m/s)	Pressure (mm Hg)	Wall Shear Stress (Pa)	Velocity (m/s)	Pressure (mm Hg)	Wall Shear Stress (Pa)
0.55	2.3973	120.742	222.729	2.3973	120.742	222.729
0.6	3.1619	130.502	341.892	3.1619	130.502	341.892
0.65	2.7651	123.616	278.35	2.7651	123.616	278.35
0.7	1.3913	106.13	90.348	1.3913	106.13	90.348
0.75	0.7487	102.631	35.233	0.7487	102.631	35.233
1	0.7655	102.651	36.33	0.7655	102.651	36.33

This similarity in the results of the two blood models is due to the fact that at high shear rates, Carreau blood model behaves as a Newtonian fluid [Sun, Xu (2014)]. It is also worth to mention here that at high shear rates, approximately all non-Newtonian models of blood behaves as a Newtonian fluid [Perktold, Hofer, Rappitsch et al., (1997)]. It can be concluded here, that assumption of blood as a Newtonian fluid in the arteries where shear rate is high can be valid. However, many previous studies have suggested that at low shear rates or low inlet velocities, blood behaves as a non-Newtonian fluid and during a cardiac cycle, there comes a point when shear rate is below 100 s^{-1} or inlet velocity is very low (less than 0.05 m/s) [Banks, Bressloff (2007)]. In the present results throughout the cardiac cycle, there is no point where blood is behaving as a non-Newtonian fluid. It could be due to the fact, that in the presented case, the assumed cardiac cycle profile is for the condition of moderate exercise with the rapid heartbeat of 120 per minute. During the whole cycle, inlet velocity ranges from 0.1 m/s to 0.5 m/s which corresponds to shear rates of 150 s^{-1} - 750 s^{-1} . Hence, it is worth to perform transient simulations with an inflow profile which incorporates the instants of low shear rate during a cardiac cycle. This work will give an insight whether assumption of blood as a Newtonian fluid under transient state for low inlet velocities is valid?

3.2.2 Newtonian vs non-Newtonian model for steady flow

A series of steady state simulations were performed for each of the three arteries and for each of the two blood viscosity models. The inlet velocity was taken to be 0.36 m/s.

The plots of WSS, pressure and velocity distributions for two of the blood models are presented for artery C in Figs. 12-14. It can be observed (Figs. 12-14) that the pattern of plots is similar for the two blood models. However, the magnitude of the maximum values attained by these flow parameters differs slightly for the two blood models (for all three arteries) as presented in Table 2. The difference between the results of two blood models is even less than 5 % which is negligible. For inlet velocity of 0.36 m/s this result is not surprising, as Carreau model tends to the Newtonian model at high shear rates. As the inlet velocity increases, magnitude of the flow parameters becomes similar for the two blood models and are almost indistinguishable.

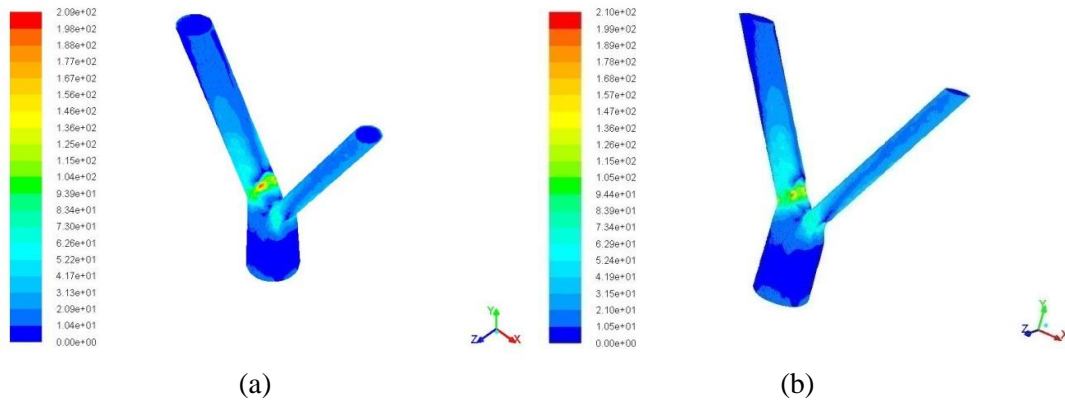


Figure 12: Distribution of wall shear stress in artery C for steady flow ($v = 0.36$ m/s) for (a) Newtonian (b) non-Newtonian models of blood

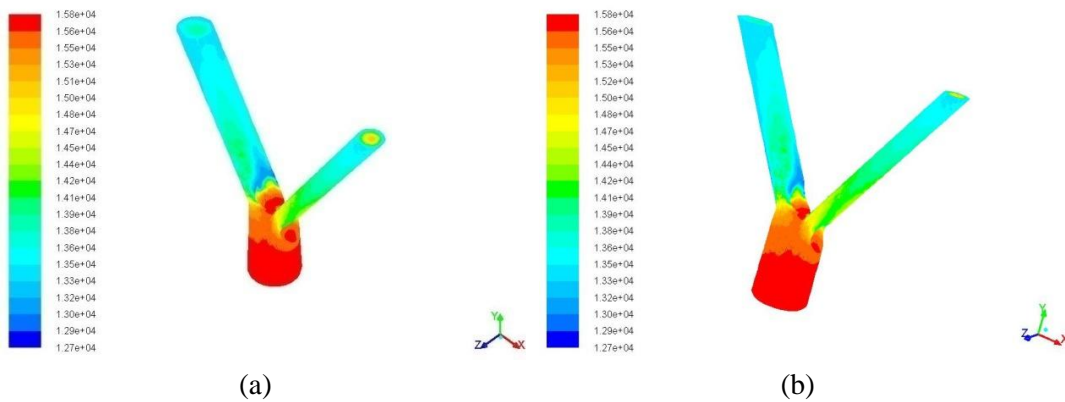


Figure 13: Distribution of pressure in artery C for steady flow ($v = 0.36$ m/s) for (a) Newtonian (b) non-Newtonian models of blood

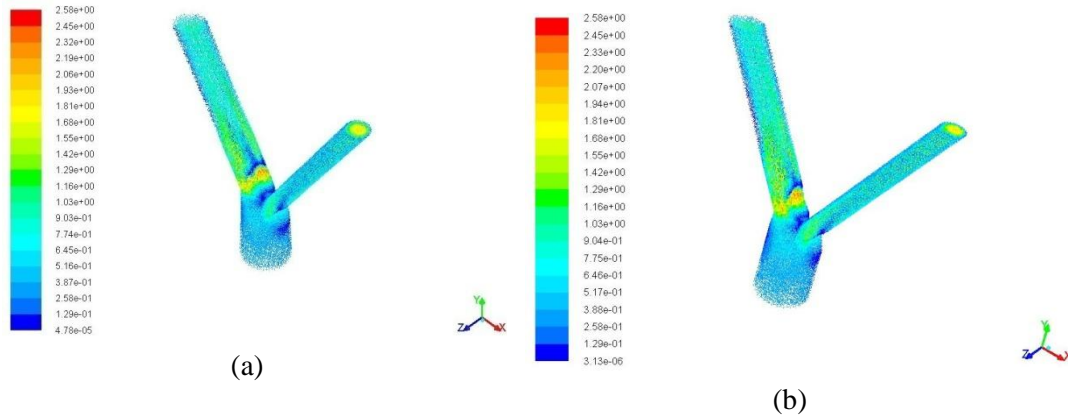


Figure 14: Distribution of velocity in artery Cover steady flow ($v = 0.36$ m/s) for (a) Newtonian (b) non-Newtonian models of blood

Table 2: Maximum values attained by flow parameters for the two blood models in steady flow.

Artery Models	V = 0.36 m/s					
	Newtonian			Non-Newtonian		
	Velocity (m/s)	Pressure (mm Hg)	Wall Shear Stress (Pa)	Velocity (m/s)	Pressure (mm Hg)	Wall Shear Stress (Pa)
A	1.2965	107.32	43.4475	1.2942	107.42	44.3697
B	2.3408	115.96	185.7776	2.3418	116.08	186.579
C	2.5795	118.19	208.61	2.584	118.29	209.7272

Ballyk, Steinman and Ethier [Ballyk, Steinman and Ethier (1994)] in their study found that visually, patterns of WSS for Newtonian and non-Newtonian flow was almost same, but magnitude of WSS for non-Newtonian case was greater than the Newtonian case. However, this result was obtained for low inlet velocities (0.01 m/s- 0.05 m/s), which again emphasises on the fact that blood behaves as a non-Newtonian fluid only at low inlet velocities or low shear rates.

3.2.3 Steady vs transient state

The comparison between the two states can be made if the boundary conditions are assumed similar for the two states. For these two states of simulation for non-Newtonian model of blood, all the boundary conditions are same except the inlet velocity profile. In order to get correct comparison between the two states, steady state simulations were performed for inlet velocities corresponding to the inlet velocity in transient state at first five times instances as mentioned in section 3.2.1. The velocities at these time instants are 0.36 m/s, 0.5 m/s, 0.4 m/s, 0.2 m/s and 0.1 m/s respectively. This set of velocity was selected so that effect of pulsatile nature of flow during transient state could also be

incorporated while making the comparison. The maximum value of WSS and pressure attained into the three artery models at $v = 0.36$ m/s ($t = 0.55$ s) for the two states is shown in Figs. 15-16 (trend of results at all time instants are same, so result for only a single time instant is presented here). It is clear from Figs. 15-16, that the values of hemodynamic parameters are underestimated if steady state flow is assumed. In fact, it is observed (Fig. 15) that for artery A (healthy artery) the deviation in result is negligible. However, for artery B, difference is more than 10 %. Stenosis in the artery depends on the wall shear stress [Jhunjhunwala, Padole and Thombre (2015)], so this underestimation in the values of WSS in steady state can influence the clinical decisions. It is, therefore, suggested to incorporate transient flow (pulsatile nature of blood flow) while doing CFD analysis of human arteries.

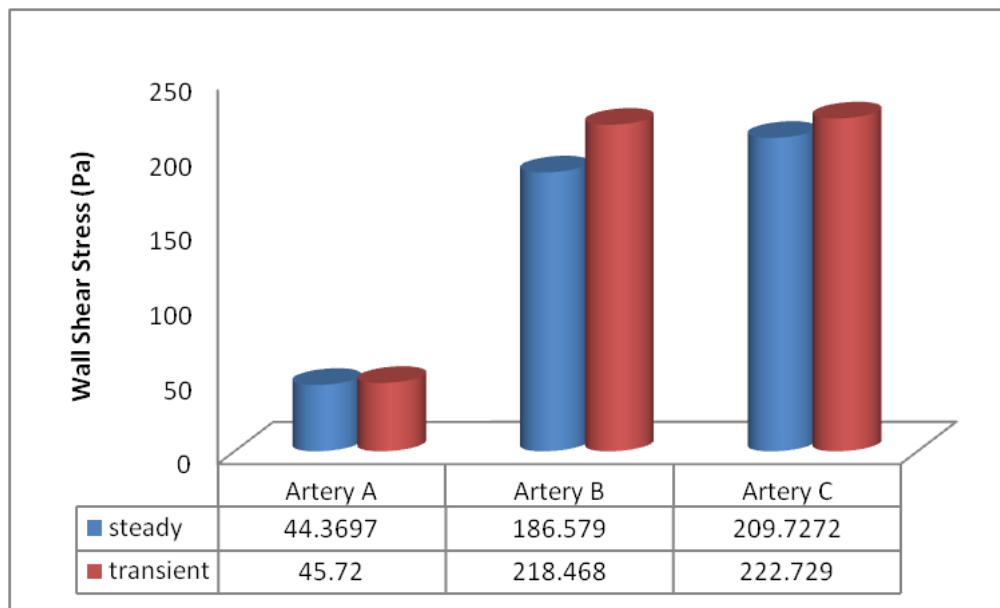


Figure 15: Comparison of maximum wall shear stress attained by the three arteries under transient ($t = 0.55$ s) and steady ($v = 0.36$ m/s) states of flow for non-Newtonian model of blood

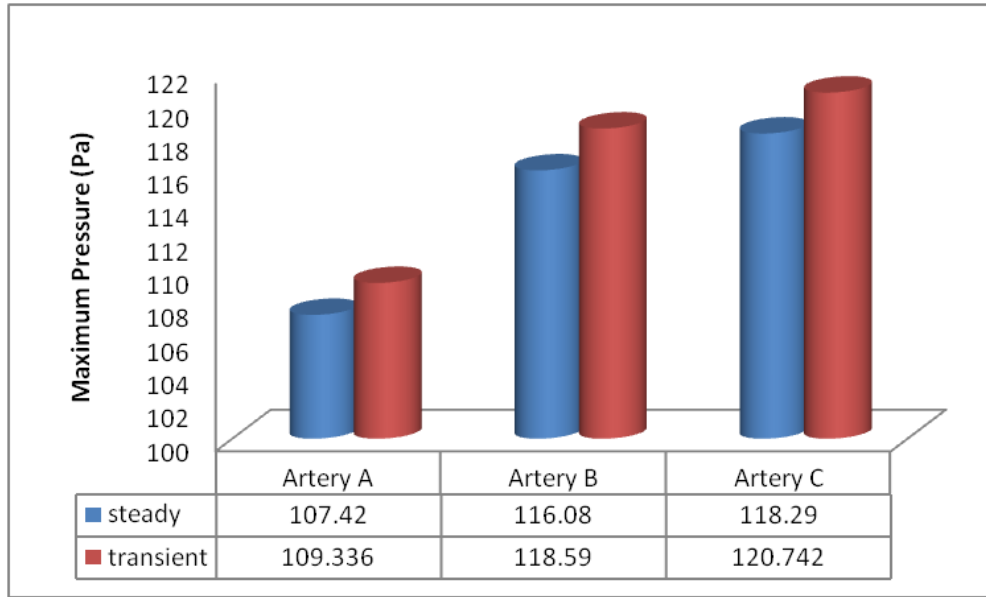


Figure 16: Comparison of maximum pressure attained by the three arteries under transient ($t = 0.55$ s) and steady ($v = 0.36$ m/s) states of flow for non-Newtonian model of blood

4 Conclusions

This paper has presented a numerical (CFD) study of blood flow through three idealized 3-D models of left coronary artery. The study has been done for two different blood viscosity models (Carreau and Newtonian) under transient as well as steady state.

The comparative study of the three artery models for non-Newtonian viscosity model of blood under transient state shows that the WSS distribution is complex and it changes significantly during a cardiac cycle. High WSS predominates at point of bifurcation for artery A (healthy artery) and at stenosed regions for artery B and C (diseased arteries). WSS, velocity and pressure increase significantly in the presence of different types of stenosis. In the post-stenotic regions, disturbances are observed in the physiological pattern of blood flow. High pressure region gets extended with increase in inlet velocity and regions of stenosis. This attributes to increase in blood pressure which is being used as indicator in clinical practice to assess the severity of stenosis.

A comparison of the two blood viscosity models for both steady and transient state shows that assumption of blood as a Newtonian fluid is a good approximation in regions of shear rates more than 100 s^{-1} . This conclusion is based on simulations for a cardiac cycle having heart rate of 120 beats per minute (during exercise) with medium-high inflow velocities. It would be interesting to see the significance of non-Newtonian model if heart rate is normal (during rest) and inflow velocity is low.

Another comparison of steady and transient flow for non-Newtonian viscosity model of

blood shows that assumption of steady flow underestimates the values of flow parameters specially WSS. It is known that WSS plays an important role in formation and growth of stenosis. It is, therefore, suggested to employ pulsatile nature of flow in numerical study of blood vessels to assess results close to real scenario.

The conclusions presented here are under assumption of idealized artery models and boundary conditions. Hence, a patient specific set up of boundary conditions and artery models can lead to more accurate results. Also, simulations were performed for a fixed mesh. However, results may show some discrepancy if simulation for elastic arterial wall and a moving artery (dynamic mesh) with beats of heart is performed.

References

Ballyk, P. D.; Steinman, D. A.; Ethier, C. R. (1994): Simulations of non-Newtonian blood flow in an end-to-end anastomosis. *Biorheology*, vol. 31, pp. 565-586.

Banks, J.; Bressloff, N. (2007): Turbulence modeling in three-dimensional stenosed arterial bifurcations. *Journal of Biomechanical Engineering*, vol. 129, pp. 40-50.

Chaichana, T.; Sun, Z.; Jewkes, J. (2011): Computation of haemodynamics in the left coronary artery with variable angulations. *Journal of Biomechanics*, vol. 44, pp. 1869-1878.

Chaichana, T.; Sun, Z.; Jewkes, J. (2013): Haemodynamic analysis of the effect of different types of plaques in the left coronary artery. *Computerized Medical Imaging and Graphics*, vol. 37, pp. 197-206.

Cho, Y. I.; Kensey, K. R. (1991): Effects of the non-Newtonian viscosity of blood on flows in a diseased arterial vessel. Part 1: steady flows. *Biorheology*, vol. 28, pp. 241-262.

Duraiswamy, N.; Schoepfoerster, R. T.; Moore, J. J. E. (2009): Comparison of near wall hemodynamic parameters in stented artery models. *J. Biomech. Eng.* vol. 131, pp. 061006 (unbound).

Gijssen, F. J. H.; Van de Vosse, F. N.; Janssen J.D. (1999): The influence of the non-Newtonian properties of blood on the flow in large arteries: steady flow in a carotid bifurcation model. *Journal of Biomechanics*, vol. 32, pp. 601-608.

Govindaraju, K.; Badruddin, I. A.; Viswanathan, G. N.; Ramesh, S. V.; Badarudin, A. (2013): Evaluation of functional severity of coronary artery disease and fluid dynamics' influence on hemodynamic parameters: A review. *European Journal of Medical Physics (Physics Medica)*, vol. 29, pp. 225-232.

Hansson, G. K. (2005): Inflammation, atherosclerosis, and coronary artery disease. *The New England Journal of Medicine*, vol. 352, pp. 1685-1695.

He, Y.; Duraiswamy, N.; Frank, A. O.; Moore, Jr. J. E. (2005): Blood flow in stented arteries: a parametric comparison of strut design parameters in three dimensions. *J. Biomech. Eng.* vol. 127, pp. 637-647.

Jeong, W.; Jaehoon, S. (2014): Comparison of effects on technical variances of computational fluid dynamics (CFD) software based on finite element and finite volume methods. *International Journal of Mechanical Sciences*, vol. 78, pp. 19-26.

Jhunjhunwala, P.; Padole, P. M.; Thombre S. B.(2015): CFD analysis of pulsatile flow and non-Newtonian behavior of blood in arteries. *Molecular & Cellular Biomechanics*,vol.12, pp. 37-47.

Johnston, B. M.; Johnston, P. R.; Corney. S.; Kilpatrick, D. (2004): Non-Newtonian blood flow in human right coronary arteries: steady state simulations.*Journal of Biomechanics*,vol. 37, pp.709-720.

Johnston, B. M.; Johnston, P. R.; Corney, S.; Kilpatrick, D.(2006): Non-Newtonian blood flow in human right coronary arteries: transient simulations. *Journal of Biomechanics*,vol. 39, pp. 1116-1128.

Karimi, S.; Dabagh, M.; Vasava, P.;Dadvar, M.;Dabir, B.;Jalali, P. (2014): Effect of rheological models on the hemodynamics within human aorta: CFD study on CT image-based geometry. *Journal of Non-Newtonian Fluid Mechanics*,vol. 207, pp. 42-52.

Kehrwald, D. (2005): Lattice Boltzmann simulation of shear thinning fluids. *Journal of Statistical Physics*,vol. 121, pp. 223-237.

Owega, A.; Klingelhofer, J.; Sabri, O.; Kunert, H. J.; Albers, M.; Sab, H. (1998): Cerebral blood flow velocity in acute schizophrenic patients: a transcranial Doppler ultrasonography study. *Stroke*,vol. 29, pp. 1149-1154.

Perktold, K.; Hofer, M.; Rappitsch, G.; Loew, M.; Kuban, B. D.; Friedman, M. H. (1997): Validated computation of physiologic flow in a realistic coronary artery branch. *Journal of Biomechanics*,vol. 31, pp. 217-228.

Pericevic, I.; Lally, C.; Toner, D.; Kelly, D. J. (2009): The influence of plaque composition on underlying arterial wall stress during stent expansion: The case for lesion-specific stents. *Med. Eng. Phys.* vol. 31, pp. 428-433.

Santamarina, A.; Weydahl, E.; Siegel Jr, J. M.; Moore Jr, J. E. (1998): Computational analysis of flow in a curved tube model of the coronary arteries: effects of time varying curvature. *Ann Biomed Eng*,vol. 26, pp. 944-954.

Sun, Z.; Cao, Y. (2011): Multislice CT angiography assessment of left coronary artery: correlation between bifurcation angle and dimensions and development of coronary artery disease. *European Journal of Radiology*,vol. 79, pp. 90-95.

Sinnott, M.; Clearly, P. W.; Prakash, M.(2006): An investigation of pulsatile blood flow in a bifurcation artery using a grid-free method. *Fifth International Conference on CFD in the Process Industries*, vol. 15, pp. 273-278.

Sun, Z.; Xu, L. (2014): Computational fluid dynamics in coronary artery disease. *Computerized Medical Imaging and Graphics*,vol. 38, pp.651-663.

Tu, C.; Deville, M. (1996): Pulsatile flow of non-Newtonian fluids through arterial stenoses. *Journal of Biomechanics*,vol. 29, pp. 899-908.

Valencia, A.; Solis, F. (2006): Blood flow dynamics and arterial wall interaction in a saccular aneurysm model of the basilar artery. *Computers and Structures*,vol.84, pp. 1326-1337.

Wellnhofer, E.; Osman, J.;Kertzsch, U.;Affeld, K.; Fleck, E.;Goubergrits, L.(2010): Flow simulation studies in coronary arteries- impact of side branches. *Atherosclerosis*,vol. 213, pp. 475-481.